Evolution of Antigen-specific T Cell Receptors In Vivo: Preimmune and Antigen-driven Selection of Preferred Complementarity-determining Region 3 (CDR3) Motifs

By Louise J. McHeyzer-Williams, Joanne Fanelli Panus, John A. Mikszta, and Michael G. McHeyzer-Williams

From the Department of Immunology, Duke University Medical Center, Durham, North Carolina 27710

Summary

Antigen (Ag)-driven selection of helper T cells (Th) in normal animals has been difficult to study and remains poorly understood. Using the major histocompatibility complex class II–restricted murine response to pigeon cytochrome c (PCC), we provide evidence for both preimmune and Ag-driven selection in the evolution of Ag-specific immunity in vivo. Before antigenic challenge, most $V\alpha11^+V\beta3^+$ Th (70%) express a critical complementarity-determining region 3 (CDR3) residue (glutamic acid at TCR-α93) associated with PCC peptide contact. Over the first 5 d of the primary response, PCC-responsive $V\alpha11^+V\beta3^+$ Th expressing eight preferred CDR3 features are rapidly selected in vivo. Clonal dominance is further propagated through selective expansion of the PCC-specific cells with T cell receptor (TCR) of the "best fit." Ag-driven selection is complete before significant emergence of the germinal center reaction. These data argue that thymic selection shapes TCR-α V region bias in the preimmune repertoire; however, Ag itself and the nongerminal center microenvironment drive the selective expansion of clones with preferred TCR that dominate the response to Ag in vivo.

Key words: immunologic memory • clonal maturation • antigen-specific immunity • helper T cells • T cell receptor

T cell recognition of peptide–MHC complexes is central to both the development of the preimmune repertoire and an adaptive immune response to foreign Ag. T cell development within the thymus involves ordered somatic rearrangement of gene elements for the TCR (1), followed by positive and negative selection of immature T cells based on TCR specificity (2, 3). These early selection events depend on TCR recognition of self-peptide–MHC complexes and serve to imprint the appropriate MHC restriction pattern on the preimmune T cell compartment (4, 5). After infection, preimmune T cells that recognize foreign peptide–MHC complexes are selected to participate in the immune response. This Ag-driven selection leads to T cell proliferation, effector cell differentiation, and the establishment of Ag-specific T cell memory (6–8). The molecular basis for these peripheral selection events and how they differ from thymic selection remains unclear.

The murine response to pigeon cytochrome c (PCC)[1] has been extensively used to study TCR peptide–MHC recognition (9). We and others have demonstrated that the majority of PCC-specific helper T cells express Vα11 and Vβ3 variable regions in their TCR, along with highly restricted sequences in the third hypervariable region (CDR3) (10–13). Jorgensen et al. (14) established critical peptide contact residues in the CDR3 loops of PCC-specific TCR (glutamic acid at α93 and asparagine at β100) that involved reciprocal charge interactions with the antigenic peptide (14). In addition, two amino acids (aa) COOH-terminal to these contact residues, serine/threonine at α95 and alanine/glycine at β102, also appear to be preferred in PCC-specific TCR (10, 11, 13). CDR3 length appears restricted in both chains of the PCC-specific TCR (8 aa for the TCR-α and 9 aa for the TCR-β), with preferred J region usage that is more apparent in the TCR-β chain (Jβ 1.2 and 2.5) than in the TCR-α chain (13). Together, these TCR features help to describe the dominant PCC-specific clonotype and provide a means for estimating TCR diversity in vivo.

The basis for clonal dominance in an adaptive immune response remains unknown. In the thymus, a diverse preimmune repertoire can be established using a single peptide–MHC complex (15–17). However, the central expression of a foreign peptide will often deplete the preimmune reper-

[1]*Abbreviations used in this paper:* aa, amino acids; CDR3, complementarity-determining region 3; GC, germinal center; LSCM, laser scanning confocal microscopic; MCC, moth cytochrome c; PCC, pigeon cytochrome c; PI, propidium iodide; RT, reverse transcriptase; TR, Texas Red.

toire of the dominant clonotype response to that peptide (17). In an adaptive response to foreign Ag, the presence of specific Th with restricted TCR structures provides strong evidence for Ag-driven selection. Our earlier studies of the PCC response indicate a high degree of restriction in the TCR of primary responders to PCC (on day 6) (13). 70% of the primary responders already had many of the CDR3 motifs associated with PCC specificity, but the frequency increased to 95% in the memory response (on day 6), suggesting further narrowing of the repertoire. It was not clear when or how this repertoire narrowing occurred. Zheng et al. indicate a rapid and progressive selection in the splenic response to PCC that is largely complete by day 12 after Ag priming (18). Similar studies in the class I–restricted T cell response to allopeptides indicate no change in CDR3 diversity of the TCR-β repertoire between the peak of the primary response and the memory response (19). Similarly, using tetramers of peptide–class I MHC, Busch and colleagues demonstrate a coordinate expansion of peptide-specific T cells (20) without particular restriction in TCR-β chain usage (21). These workers suggest a further narrowing of the TCR repertoire upon secondary stimulation (22), which is not seen in other class I–restricted responses (21, 23). Although these studies are not necessarily contradictory, they highlight the need for more comprehensive molecular analysis of the early developing phase of the immune response.

Ag-specific Th are difficult to visualize in normal animals. Jenkins and colleagues adoptively transferred TCR-transgenic Th of known specificity into normal recipients to monitor the dynamics of the specific T cell response (24, 25) and, more recently, cognate T–B cell interactions (26). Their studies document the transition of Ag-specific T cells from clusters associated with dendritic cells in the T cell zones (27) to the B cell areas of secondary lymphoid organs (26). In conventional animals, the Vα11Vβ3-expressing T cells also initially expand in the T cell zones of a splenic response to PCC (18, 28). The later phase of the PCC-specific response is characterized by the germinal center (GC) localization of Vα11Vβ3-expressing T cells (18, 28). In repertoire studies, Zheng et al. (18) demonstrated that the Vα11Vβ3-expressing cells in GC have more restricted CDR3 loops than their T cell zone counterparts. Furthermore, the GC Th were highly sensitive to TCR- and steroid-induced apoptosis in vivo (18).

In this study, we assessed changes in TCR diversity during the emergent phase of the primary and memory response to PCC in nontransgenic animals. We directly analyzed CDR3 sequences from single, PCC-specific Th ($CD8^-B220^-CD11b^-V\alpha11^+V\beta3^+CD44^{hi}CD62L^{lo}$) at various timepoints throughout the immune response and compared them to the preimmune repertoire. The memory response emerged highly restricted (days 2, 3, and 4), with eight distinguishing CDR3 features in the majority of PCC-specific cells. Only one of these features, a glutamic acid at the V–J border (α93), appeared in the preimmune repertoire at high frequencies (70% of Vα11Vβ3-expressing Th). By day 3 of the primary response, 40% of PCC-specific cells expressed a restricted TCR containing at least six of the eight preferred CDR3 features. Ag-driven selection in the primary response was complete by day 5, when 80% of the PCC-specific compartments expressed restricted TCR. The frequency of PCC-specific T cells with restricted receptors remains ~80% to the end of the second week after Ag priming but increased to 96% in the memory response. In situ analysis indicated that GC are only beginning to form on day 5, with very few PCC-specific Th present in the GC at this stage. Overall, these data suggest that the Vα11 bias that dominates the PCC response is centrally imposed before antigenic challenge. After initial priming, Ag and the non-GC microenvironment selectively expand Vα11Vβ3-expressing Th with preferred CDR3 features that dominate the primary immune response and establish Ag-specific Th memory.

Materials and Methods

Mice and Immunization

6–10-wk-old, male B10.BR mice were purchased as specific pathogen free from The Jackson Laboratory and housed under reverse barrier conditions at the Duke University Vivarium until they were killed. Whole PCC (Sigma Chemical Co.) was diluted into PBS and mixed with the Ribi adjuvant system (Ribi Immunochem Research). Primary immunization of 400 μg of PCC was injected into 200 μl of adjuvant emulsion in two 100-μl doses subcutaneously on either side of the base of the mouse tail. PBS alone was used for the adjuvant-only controls. The memory challenge was designed as a second primary immunization to reduce the differences between the two responses (i.e., no dose differences to account for changed kinetics of the cellular response). Secondary challenge was a repeat of the primary regime including adjuvant, also at the base of the tail, 8 wk after the initial priming.

Flow Cytometry

Animals were killed on various days after immunization as indicated, and the draining LNs were harvested for analysis. Inguinal and periaortic nodes were collected and teased through 80-μm mesh screens into single-cell suspensions in 0.17 M NH_4Cl solution for erythrocyte lysis before estimation of cell count using a hemocytometer. Cells were pelleted and resuspended in PBS with 5% FCS. All cells were stained for flow cytometry at 2.0×10^8 cells/ml with predetermined optimal concentrations of fluorophore (or biotin)-labeled mAb (FITC–RR8.1 [anti-Vα11; PharMingen], allophycocyanin–KJ25 [anti-Vβ3], PE–Mel14 [anti-CD62L; PharMingen], Cy5PE–6B2 [anti-B220; PharMingen], Cy5PE–53-6.7 [anti-CD8; PharMingen], Cy5PE–M1/70.15 [anti-CD11b; Caltag Labs.], or biotin–IM7 [anti-CD44; PharMingen]) together with desired volume of cells on ice for 45 min. After being washed twice, cells were resuspended at the same cell concentration with avidin–Texas Red (TR; PharMingen) on ice for 15 min, washed again, and resuspended in 2 μg/ml propidium iodide (PI) (for dead cell exclusion) in PBS with 5% FCS for analysis.

Samples were analyzed using a dual laser, modified FACStar$^{PLUS™}$ (Becton Dickinson Immunocytometry Systems) (an argon laser as the primary and a tunable dye laser as the secondary) capable of seven-parameter simultaneous collection (five log-amp detectors for fluorescence, one log-amp detector for obtuse light scatter, and a photo diode for forward light scatter). The Cy5

component of the duochrome Cy5PE is also excited by the dye laser and detected in the allophycocyanin channel. For all experiments described, the Cy5PE fluorescence collected after primary laser excitation was used for exclusion criteria alone (see Fig. 1 A), thereby operationally avoiding the signal overlap across the two lasers that could not be compensated for electronically. PI was also excluded in the Cy5PE detection channel. All analyses required the collection of two files for each sample. The first file was a 100,000-event file of PI^- events to ascertain the frequency of $Cy5PE^-$ $V\alpha11V\beta3$-expressing cells in the total LN population. The second file contained 1,000 events of PI^-Cy5PE^- $V\alpha11^+V\beta3^+$ cells to evaluate the fraction of cells that upregulated CD44 and downregulated CD62L. Files were acquired using CELLQuest™ software (Becton Dickinson) and analyzed using FlowJo software (Tree Star, Inc.). All profiles are presented as 5% probability contours with outliers. Total cell numbers were calculated using frequencies estimated by flow cytometry and total cell counts for the draining LNs of each animal.

Laser Scanning Confocal Microscopy

Draining LNs used for confocal microscopy were snap frozen in OCT embedding compound (Miles Labs., Inc.). Cryostat microtome (Leica, Inc.) cut, 6-μm-thick frozen sections were mounted on gelatin-coated slides, air dried, and acetone-fixed for 10 min at 4°C and stored at −80°C until use. Sections were rehydrated with PBS and blocked with PBS containing 10% FCS, 10% skim milk (wt/vol) powder, and 2.4G2 (anti-FcR) (50% vol/vol hybridoma supernatant) for 30 min at room temperature. Sections were stained with TR-11.26 (anti-IgD), allophycocyanin–KJ25 (anti-Vβ3), and either FITC–RR8.1 (anti-Vα11) or FITC–Mel14 (anti-CD62L) for 1 h at room temperature, then washed and mounted in VectorShield (Vector Labs., Inc.). FITC is excited at 488 nm and collected using a 515–545-band pass filter, TR is excited at 568 nm and collected using a 615–645-band pass filter, and allophycocyanin is excited at 633 nm and collected using a 670–810-band pass filter. Data was acquired on a Zeiss Axiovert LSM 410 microscope system (Carl Zeiss, Inc.), and each image was collected serially in the first detector, using LSM 3.95 software. Quantitation was achieved manually after digital rendering of the image for optimal signal-to-noise and overlay using Adobe Photoshop (Adobe Systems, Inc.). Single $V\alpha11^+$ and $V\beta3^+$ cells were first counted separately (and then overlapping), using a grid covering each field (acquired using the 40× objective lens), covering one full section of the LN. The IgD staining was then used to assign each cell's location—T zone (mainly IgD^-), B zone (mainly IgD^+), or GC (IgD^- area within the B cell zone)—as well as exclude nonspecific staining (positive for all three signals). Sections containing both T zone and B zone areas were used for analysis.

Single-Cell Repertoire Analysis

cDNA Synthesis. Single cells with appropriate surface phenotype were sorted for repertoire analysis using the automatic cell dispensing unit attached to the FACStar$^{PLUS™}$ and Clone-Cyt™ software (Becton Dickinson). Each cell was sorted into an oligo d(T)-primed, 5-μl cDNA reaction mixture (4 U/ml murine leukemia virus–RT [GIBCO BRL] with recommended 1× RT buffer, 0.5 nM spermidine [Sigma Chemical Co.], 100 μg/ml BSA [Boehringer Mannheim], 10 ng/ml oligo d(T) [Becton Dickinson], 200 μM each dNTP [Boehringer Mannheim], 1 mM dithiothreitol [Promega Corp.], 220 U/ml RNAsin [Promega Corp.], 100 μg/ml *Escherichia coli* tRNA [Boehringer Mannheim], and 1% Triton X-100) set up in low profile, 72-well microtiter trays (Robbins Scientific), immediately held at 37°C for 90 min, and then stored at −80°C until further use.

Single cells were only sorted into the center 60 wells of each tray, with the first and last well of each row serving as a negative control (processed together with all other samples throughout the experimental procedure). These negative controls are critical to ascertain the efficacy of the "nested" PCR to follow (one negative for each five samples). Single hybridoma cells can be sorted into medium in these trays and visualized under a phase-contrast microscope to test the accuracy of sorting into these small format wells and demonstrated an accuracy range of 60–80% single cells (doublets never seen). A nested RT-PCR for actin mRNA serves as a more sensitive positive control for sorting and produces a PCR product for 70–100% of wells with a sorted cell.

Nested PCR: First Rounds of PCR (PCR-a). 2 ml of cDNA from single-cell cDNA reactions were used for two separate, 25-μl amplification reactions, one for the TCRVα11 and one for the TCRVβ3, using primers specific for the V and constant regions of each chain (2 U/ml Taq polymerase with the recommended 1× reaction buffer [Promega Corp.], 0.1 mM of each dNTP [Boehringer Mannheim], and for [a], TCRVα11, 2 mM $MgCl_2$, 1.2 μM primer Vα11.L1 [5′-ATGCAGAGGAACCTGGGAGC-3′] and 1.2 μM primer Cα.2 [5′-AATCTGCAGCGGCACATTGATTTGGGA-3′]; [b], TCRVβ3, 3 mM $MgCl_2$, 0.4 μM primer Vβ3.L2 [5′-ATGGCTACAAGGCTCCTCTGGTA-3′], and 0.4 μM primer Cβ.2 [5′-CACGTGGTCAGGGAAGAA-3′]). Each reaction set begins with 95°C for 5 min; then 40 cycles of 95°C for 15 s, 50°C for 45 s, and 72°C for 90 s; and ends with 72°C for 5 min.

Second Rounds of PCR (PCR-b). 1 μl of the first PCR product was used for further 25-μl amplification reactions for each chain of the TCR, using primers nested medially to the primers used in PCR-a (2 U/ml Taq polymerase with the recommended 1× reaction buffer [Promega Corp.], 0.1 mM of each dNTP (Boehringer Mannheim), and for [a], TCRVα11, 2 mM $MgCl_2$, 0.8 μM primer Vα11.L2 [5′-AATCTGCAGTGGGTGCAGATTTGCTGG-3′] and 0.8 μM primer Cα.ext [5′-GAGTCAAAGTCGGTGAACAGG-3′]; and [b], TCRVβ3, 4 mM $MgCl_2$, 0.4 μM primer Vβ3.1 [5′-AATCTGCAGAATTCAAAAGTCATTCA-3′], and 0.4 μM primer Cβ.3 [5′-AATCTGCAGCACGAGGGTAGCCTTTTG-3′]). Each reaction set begins with 95°C for 5 min; then 35 cycles of 95°C for 15 s, 55°C for 45 s, and 72°C for 90 s; and ends with 72°C for 5 min.

At least 2 negative cDNA samples were processed per 10 single-cell samples. The negatives were interspersed with positives to control for contamination during sample preparation. Frequency for obtaining a sequenceable PCR product from single cells varies between TCR-α and TCR-β (primarily due to lower abundance of TCR-α mRNA per cell), with some variation across different days in the response (Table I).

DNA Sequencing. 5 μl of PCR-b product was run on a 1.5% agarose gel to screen for positives (single bands of the right size). PCR product was then separated from primers using a CL-6B Sepharose column (Pharmacia LKB Biotechnology, Inc.). The

Table I. *Single-Cell PCR Efficiency*

	Week 1	Week 2	Memory	Total
TCR-α	35 ± 3%	49 ± 11%	43 ± 2%	44 ± 4%
TCR-β	69 ± 3%	78 ± 7%	66 ± 5%	71 ± 3%

PCR product was then directly sequenced (3 μl of PCR product, 4 μl Dye Terminator Ready Reaction Mix [Perkin Elmer Corp.], 1.5 pmol primer [Vα11.seq, 5′-CAGGAACAAAGGAGAAT GGGAG-3′; Vβ3.seq, 5′-CTGTGCTGAGTGTCCTTCAAAC-3′]) using a linear amplification protocol for 25 cycles of 96°C for 10 s, 50°C for 5 s, and 60°C for 4 min on a 9600 GeneAmp PCR system (Perkin Elmer Corp.). Samples were separated on a 6.5% acrylamide gel after ethanol precipitation of sequencing reaction products, run on an ABI 373 sequencing system, and processed using ABI Prism sequence 2.1.2 for collection and analysis (Perkin Elmer Corp.).

Results

Quantitation and Isolation of the PCC-specific Th Response. To purify the PCC-specific subset, we isolated Vα11Vβ3-expressing $CD4^+$ cells that modulate surface CD44 and CD62L (l-selectin) expression in response to Ag. Fig. 1 A outlines our flow cytometric strategy for purifying PCC-specific cells, using seven cellular parameters simultaneously. This new strategy significantly decreases background to allow more confident cell sorting, even at extremely low target cell frequencies ($<1/10^4$ cells on day 3). The initial background of Vα11Vβ3-expressing cells that are also $CD44^{high}CD62L^{low}$ is negligible before immunization (Fig. 1 A, panel iv). In the absence of protein Ag, not only on day 3 but also through to day 7, there is negligible appearance of Ag-responsive cells (Fig. 1 B, top row). There is a significant difference between adjuvant-only versus day 3 PCC-responsive cells ($P = 5.0 \times 10^{-4}$) (Fig. 1 C). In addition, the response to an irrelevant protein, such as hen egg lysozyme, is similarly low (data not shown). These critical in vivo controls attest to the specificity of cells responding to PCC.

The increase in frequency for Ag-responsive Vα11Vβ3 cells ($CD44^{hi}CD62L^{lo}$) is depicted in the probability contours of Fig. 1 B. It is important to note that the total cellularity of the draining LNs also changes over the course of the immune response. Therefore, it is more informative to consider the change in total cell numbers of Ag-responsive cells over the course of the response (Fig. 1 C). We observed a 250-fold increase in cell numbers between days 0 and 7 of the primary response. Of course, the fidelity of the day 0 quantitation is limited by detection and not the actual precursor frequency in the preimmune repertoire. There is an apparent plateau in cell numbers from days 7 to 9 of the primary response and then a gradual decline. The extent of the cellular response to the secondary challenge with the same dose of Ag is very similar to the primary response. It is the accelerated kinetics of this cellular response that highlights one of the unique characteristics of a memory Th response (peak on day 3; Fig. 1, B and C) (13).

The Memory Response Emerges Highly Restricted. Using the flow cytometric strategy outlined above, we can isolate single PCC-responsive cells from the emergent phase of both the primary and memory response to Ag. We first focus our attention on the memory response. We had previously defined the expression of highly restricted TCR on day 6 of the memory PCC response (13). It was not known whether the restricted TCR expressed on day 6 were the result of clonal maturation following secondary challenge. Therefore, we isolated single cells from days 2, 3, and 4 for repertoire analysis, as described in detail in Materials and Methods. Regardless of the day after challenge, TCR expressed by memory response cells are highly restricted (sequences from days 2 and 4 are displayed in Fig. 2). The similarity between aa sequences from different cells can be easily seen; however, clonal relatedness can only be established by comparing DNA sequences of both TCR-α and TCR-β chains from single cells. Identical sequences for both chains were seen in only 6/46 TCR sequences from the memory response (across four separate animals). These repeat sequences were not amplification artifacts (which are rigorously scrutinized in the experimental design) and therefore represent examples of single cells from the same parent clone in vivo. Overall, these data demonstrate that the memory response to PCC emerges rapidly, using a broad array of memory–response precursor cells that already express highly restricted TCR.

Using this more complete data set, we can define four preferred CDR3 features (in each chain of the TCR) that typify the PCC-specific memory Th compartment. In the TCR-α chain (Fig. 2): (i) glutamic acid (E) at α93; (ii) CDR3 length of 8 aa; (iii) serine (S) at α95; and (iv) Jα 16, 17, 22, and 34. In previous studies, a threonine was also seen at α95, but it was not seen in this study (0/51 TCR-α chains). We can now assign Jα 16, 17, 22, and 34 as preferred, with each Jα used by >10% of the memory responders and together accounting for 70% of memory responders. These four Jα can produce a serine at position α95 given the appropriate V–J junction; however, the four Jα represent only a subset of total Jα segments that can create this serine (at least 10 others). Therefore, the Jα segments are preferred for reasons other than simply the creation of a serine at α95. The four preferred features in the TCR-β chain are: (i) asparagine (N) at β100, (ii) CDR3 length of 9 aa, (iii) alanine (A) or glycine (G) at β102, and (iv) Jβ1.2 and Jβ2.5. The β102 position is considered separately from the Jβ1.2, as most often, the alanine appears to be lost in D–J joining in the preimmune repertoire (4/13 Jβ1.2 expressing preimmune TCR retain the alanine, and only two of these express the alanine at the correct position). Therefore, Jβ1.2 is not the preferred motif but rather a Jβ1.2 that retains an alanine at position β102. A glycine is also found in the β102 position when Jβ2.5 is used. In these cases, the glycine is encoded by D region or N sequence insertions and is not present in the germline Jβ2.5.

Glutamic Acid at α93 Preexists Ag Challenge. To evaluate when the dominant clonotype emerges, we next sorted single PCC responder cells from throughout the primary response. The dot plot displays in Fig. 3, A–D and Fig. 4, A–D summarize the CDR3 sequence information for either the TCR-α or TCR-β chains from over 500 single cells. Each dot represents the sequence from a single cell, and each of the eight CDR3 features from these cells are displayed separately. The preferred CDR3 motif is pre-

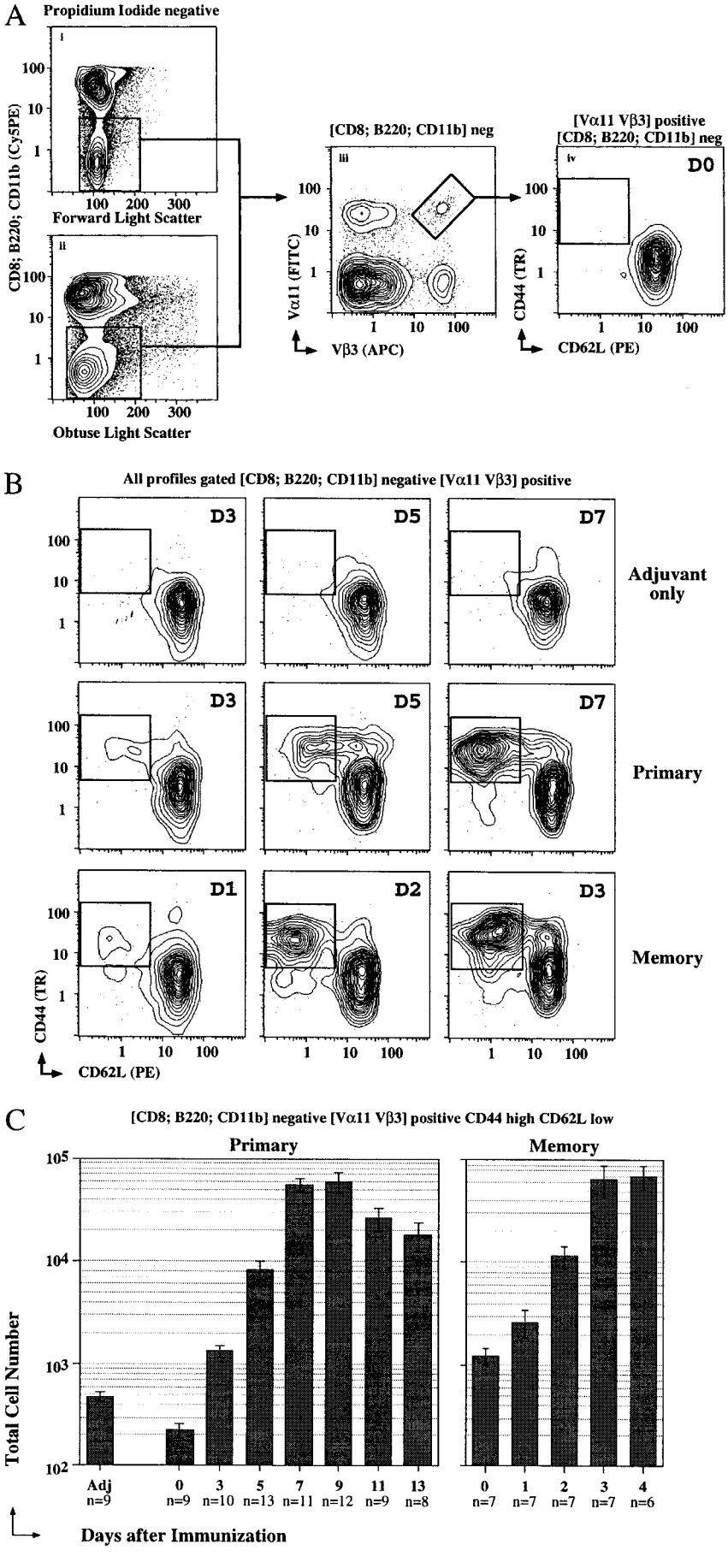

Figure 1. Five-color flow cytometric identification of PCC-specific Th. (A) Seven-parameter flow strategy outlined sequentially. Cells were stained using FITC–RR8.1 (anti-Vα11), allophycocyanin–KJ25 (anti-Vβ3), PE–Mel14 (anti-CD62L), Cy5PE–6B2 (anti-B220), Cy5PE–53-6.7 (anti-CD8), Cy5PE–M1/70 (anti-CD11b), TR–avidin/biotin–IM7 (anti-CD44), and PI as described in Materials and Methods. (i and ii) PI is excluded using the Cy5PE channel at acquisition, and cells positive for CD8, B220, and CD11b are also excluded using Cy5PE. Forward and obtuse light scatter are set to exclude many macrophages and most neutrophils but include T cell blasts. (iii) Vα11 and Vβ3 staining allows isolation of non-CD8 T cells that express both chains of the receptor shown in the insert of this panel. (iv) CD44 and CD62L levels on the T cells with TCR, using the V regions preferred for PCC specificity before injection. (B) Representative probability contours for CD44 and CD62L expression on Vα11Vβ3-expressing T cells. The day after Ag administration is displayed in the upper right of each panel, over the course of the primary response with adjuvant only (top row), primary PCC response (middle row) and memory response (bottom row). The insert box indicates the limits of CD44 upregulation and CD62L downregulation that were used to calculate frequencies of cells that respond to Ag. (C) Frequencies of Vα11Vβ3-expressing T cells that have upregulated CD44 and downregulated CD62L and total cell numbers from each animal calculated at the time animals were killed are used to estimate the change in total Ag-responsive cells in the draining LNs during the course of the primary and memory response. Varying numbers of single animals were used as indicated by the *n* below each time-point on the x-axis, with means ± SEM displayed. There was no significant difference in the adjuvant-only response across different days, and it is presented together from day 3 (×2), day 5 (×2), and day 7 (×5). Significant differences (2-tail *t* test) are observed: in the primary response, between days 0 and 3 ($P = 3.0 \times 10^{-5}$), days 3 and 5 ($P = 3.0 \times 10^{-3}$), days 5 and 7 ($P = 10^{-6}$), adjuvant-only full data set day 3 ($P = 5.0 \times 10^{-4}$); and in the memory response, between days 0 and 2 ($P = 10^{-2}$), days 2 and 3 ($P = 4.0 \times 10^{-2}$).

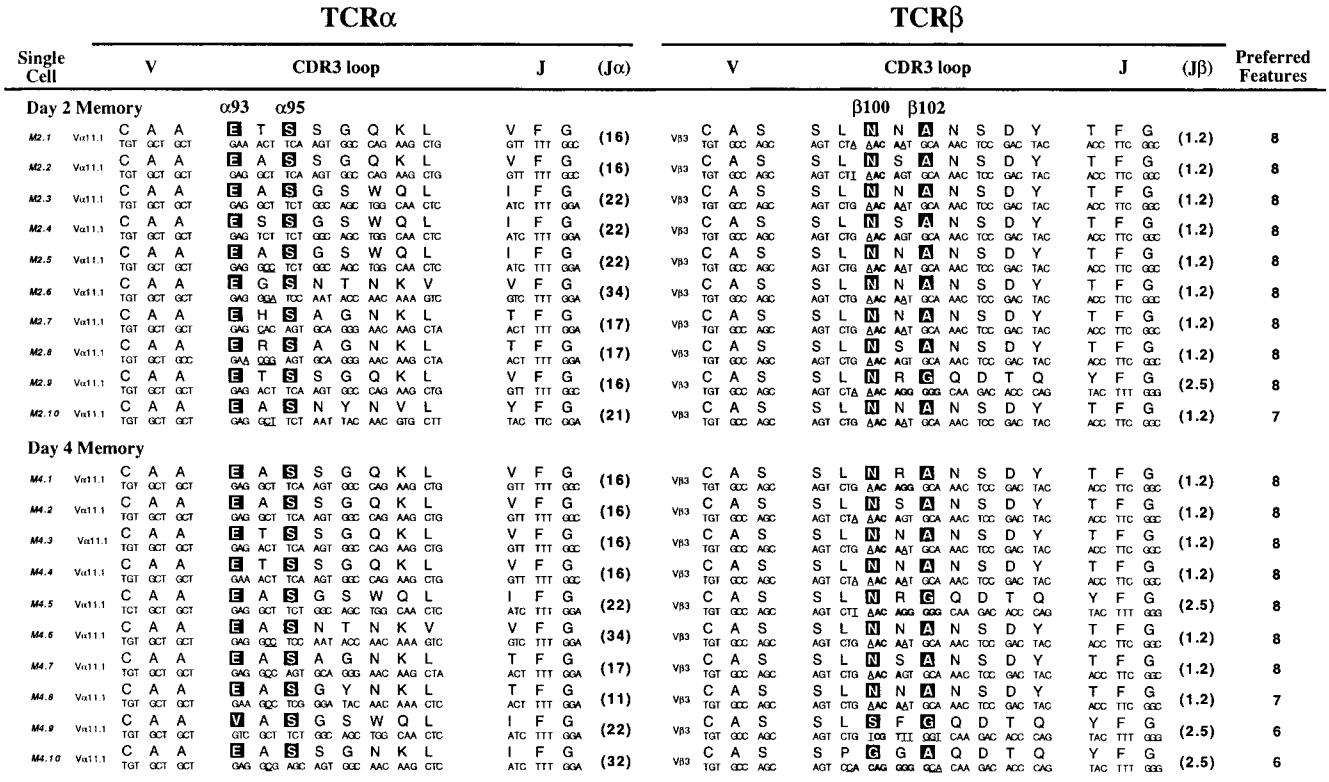

Figure 2. PCC-specific memory cells emerge with highly restricted TCR. Single PCC-specific T cells were sorted into cDNA reaction mix, subjected to two separate rounds of PCR for TCRVα11 and TCRVβ3, and then cycle-sequenced, focusing primarily on the CDR3 region of each chain from days 2 and 4 of the memory response, as indicated. A representative set of nucleotide and predicted aa sequence from single T cells where both chains of the TCR were analyzed. The TCR-α aa positions α93 and α95 and, in the TCR-β, aa positions β100 and β102, are highlighted in each sequence. The TCRJ region usage is displayed, with the CDR3 length presented between the V and J elements not considered as part of the loop (2 aa downstream from the conserved C and 2 aa upstream from the conserved GXG in the TCRJ). The N sequence in each chain is underlined, and the D region in the TCR-β chain is in bold. The preferred features column refers to the CDR3 features predominant in PCC-specific hybridoma and those which appear repeatedly in the memory response to this Ag (TCR-α: E at α93; S at α95; length of 8 aa; and TCRJα 16, 17, 22, and 34. TCR-β: N at β100; A/G at β102; length of 9 aa; and TCRJβ 1.2 and 2.5). A, alanine; E, glutamic acid; G, glycine; N, asparagine; S, serine.

sented at the top of each panel, with alternative features displayed in order of prevalence. A summary for each chain in Figs. 3 E and 4 E combines all CDR3 features from individual animals to demonstrate when the repertoire narrows over the course of the developing immune response.

Considering all eight preferred CDR3 features, only the glutamic acid at α93 preexists antigenic challenge to any significant extent (Fig. 3 A). In preimmune and PCC-nonresponsive Th ($V\alpha11^+V\beta3^+CD44^{lo}CD62L^{hi}$), 68% express glutamic acid at position α93 ($n = 62$). In the same population, the three other preferred TCR-α chain features are present in <30% of the cells (Fig. 3, B–D). The glutamic acid at α93 is encoded by the last codon of the V region and may be lost on imprecise V–J joining. Its presence in the preimmune repertoire may be simply stochastic or the result of thymic selection pressures. Greater than 90% of all Vα11Vβ3-expressing T cells in the periphery of normal B10.BR mice are $CD4^+$, implicating thymic selection and MHC class II restriction as a defining characteristic of the preimmune repertoire for these particular T cells (data not shown) (13). Of 75 murine TCR-α regions listed by Arden et al. (29), only four can express a germline-encoded glutamic acid at α93. All four V regions are Vα11 subfamily members. Therefore, it seems likely that the presence of this one critical peptide contact residue that preexists antigenic challenge at very high frequencies in the Vα11Vβ3-expressing Th imposes the TCR-α chain V region bias of the I-E^k–restricted PCC response.

Evidence for Clonal Maturation in Each Chain of the TCR. The remaining seven preferred CDR3 features are rapidly selected during the cellular expansion phase of the primary response (days 3–7; doubling time of the population was 17.5 h). Even by day 3 of the primary response, there is an accumulation of Ag-activated Vα11Vβ3 cells with many of the preferred CDR3 features (Fig. 3, B–D and Fig. 4, A–D). There is a large spread of Jα usage in the PCC-nonresponsive cells that has already narrowed by day 3 (35%) and narrows further (65%) to use the four preferred Jαs by day 5 (Fig. 3 B). The CDR3 lengths of 8 and 9 aa are most prevalent in the PCC-nonresponsive cells; however, the preference for a length of 8 aa in the PCC-specific compartment is evident even by day 3 and maximal by day 5 (Fig. 3 C). Selection for serine at α95 also appears maximal by day 5 of the primary response (Fig. 3 D).

Many PCC-specific hybridomas contain at least three out of the four CDR3 features described. Therefore, in

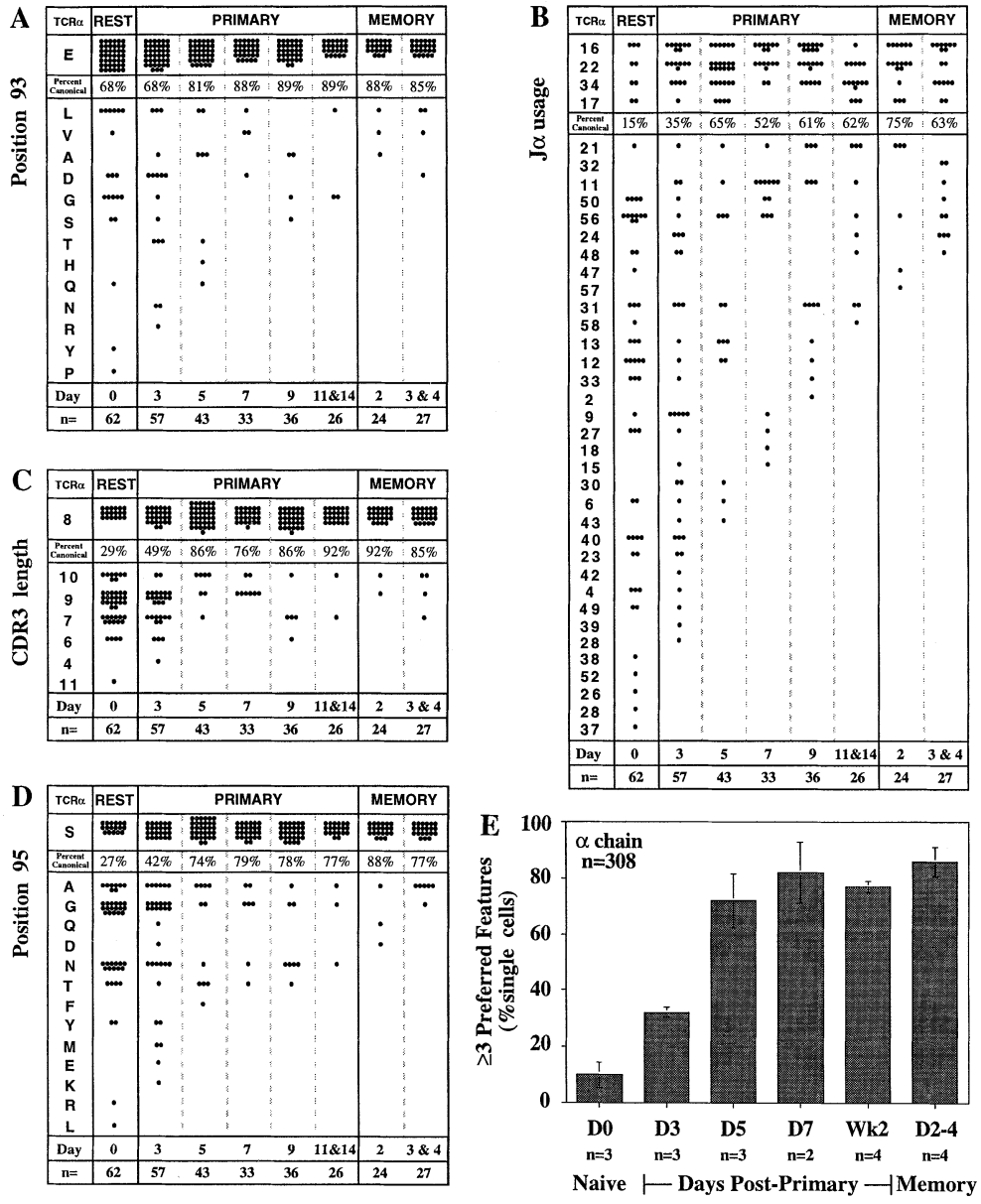

Figure 3. Ag-driven selection for preferred TCR-α CDR3 features. Single-cell repertoire analysis was undertaken as described in Materials and Methods. In A–D, the CDR3 features known to be selected in the PCC response are treated separately. A, position α93; B, TCRJα usage; C, CDR3 length; and D, position α95. Each dot represents the sequence information from a single Ag-responsive cell (after day 0), with the preferred CDR3 feature presented at the top of each panel and the percentage of single cells expressing this feature displayed in the next line as "percent canonical." Each panel organizes the information as a progression over time (from left to right) before injection (day 0, REST), after primary immunization (days 3, 5, 7, and 9 separately and 11 and 14 together), and after memory immunization (days 2, 3, and 4). The number of sequences used in the analysis are displayed as the *n* below the depicted days on the x-axis. The REST group includes Vα11Vβ3-expressing T cells before injection with a resting phenotype ($CD44^{lo}CD62L^{hi}$) ($n = 40$) and those from days 3 and 5, also with the resting phenotype ($n = 22$). Both groups contained similarly diverse TCR-α CDR3 regions, as did the few cells sampled from the adjuvant-only set on day 7 after primary injection (not shown). (E) A summary of the change in the percentage of single cells that expressed ≥3 of the preferred TCR-α CDR3 features over time during the response to PCC. These data represent a percentage for each animal analyzed (where there were ≥10 sequences) and the mean ± SEM for each timepoint (*n* below the x-axis, number of animals from which sequences were taken; $n = 308$ individual sequences used for the analysis). Significant differences (2-tail *t* test) were observed between days 0 and 3 ($P = 0.01$) and days 3 and 5 ($P = 0.01$).

Fig. 3 E, we consider the change in the frequency of cells that express ≥3 preferred CDR3 features in their TCR-α chains to assess the dynamics of clonal maturation. By day 3, there is a significant difference in cells that express ≥3 preferred features over the PCC-nonresponsive cells ($P = 0.01$, 2-tail *t* test). There is a further increase in frequency of restricted TCR by day 5 (days 3–5, $P = 0.01$) but no significant difference over the course of the primary response. This was also true between the late primary response and the memory response. Furthermore, we found no evidence for somatic diversification of the TCR-α genes (30) (no mutations observed for 5,441 bases analyzed for the TCR-α chain from days 7, 9, and 11; $n = 83$ single cells, 40–90 bp upstream of the CDR3 in each case).

A similar rapid progression of Ag-driven selection was apparent for the TCR-β chain. Very few PCC-nonresponsive cells express an asparagine at β100 (6%), with evidence for selection in the PCC-specific compartment by day 3 (20%) and clearly by day 5 (65%) (Fig. 4 A). This preferred CDR3 feature appears further selected by day 7 (73% by day 7; 78% average over days 7–14), with still further selection in the memory response (90% average over days 2–4). Preferred Jβ usage (1.2 and 2.5) follows a similar course (Fig. 4 B): a small increase in Jβ1.2 and 2.5 usage on day 3 (23% resting to 34% by day 3) that is clearly dominant by day 5 (77%), with a further increase by day 7 (88%; 88% average, days 7–14) and a slight increase in the memory response (94% average). CDR3 length restriction may be more rapid than the previous two features (Fig. 4 C). The appearance of PCC-specific cells with a 9-aa length is

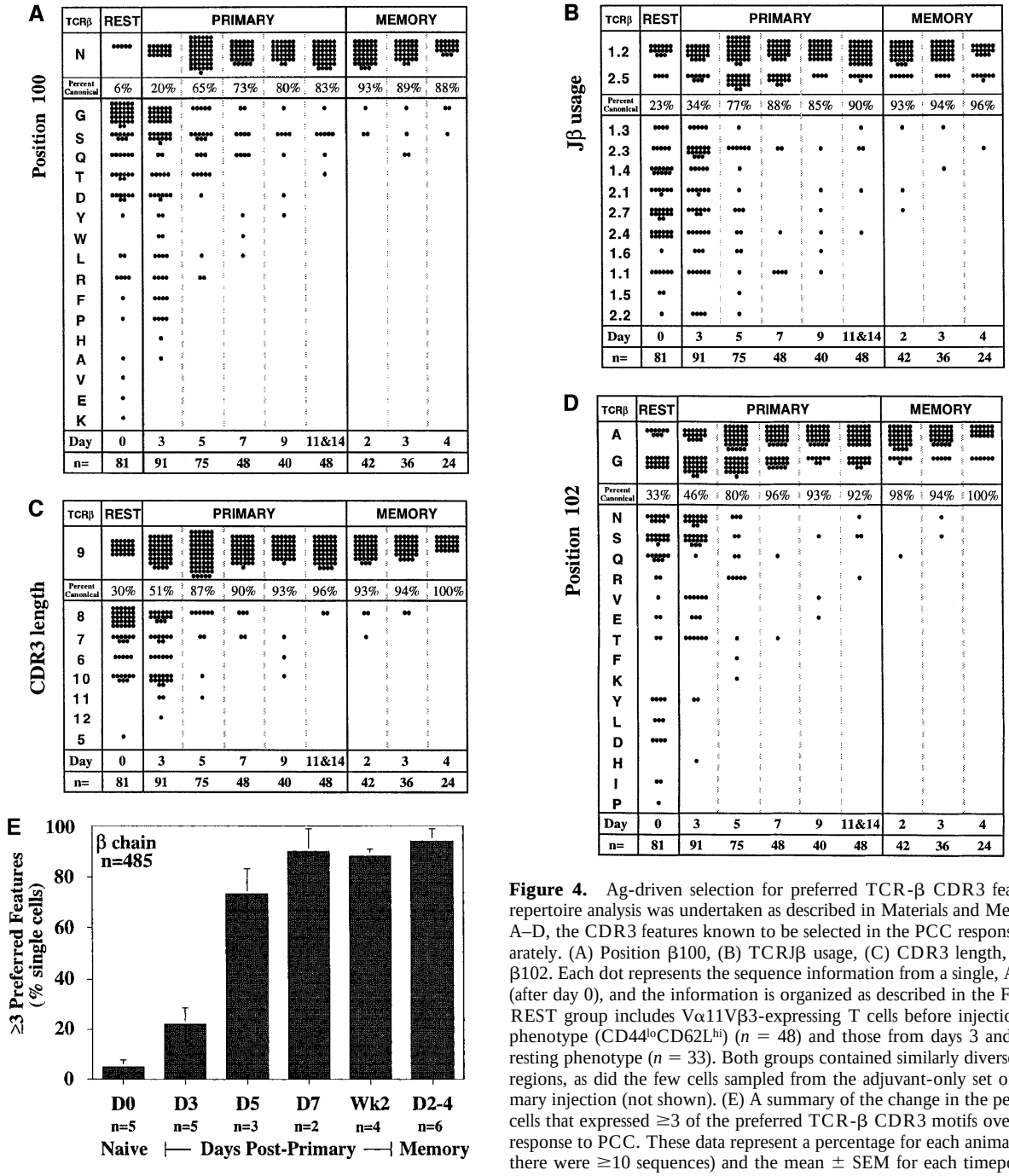

Figure 4. Ag-driven selection for preferred TCR-β CDR3 features. Single-cell repertoire analysis was undertaken as described in Materials and Methods. In sections A–D, the CDR3 features known to be selected in the PCC response are treated separately. (A) Position β100, (B) TCRJβ usage, (C) CDR3 length, and (D) position β102. Each dot represents the sequence information from a single, Ag-responsive cell (after day 0), and the information is organized as described in the Fig. 3 legend. The REST group includes Vα11Vβ3-expressing T cells before injection, with a resting phenotype ($CD44^{lo}CD62L^{hi}$) ($n = 48$) and those from days 3 and 5, also with the resting phenotype ($n = 33$). Both groups contained similarly diverse TCR-β CDR3 regions, as did the few cells sampled from the adjuvant-only set on day 7 after primary injection (not shown). (E) A summary of the change in the percentage of single cells that expressed ≥3 of the preferred TCR-β CDR3 motifs over time during the response to PCC. These data represent a percentage for each animal analyzed (where there were ≥10 sequences) and the mean ± SEM for each timepoint (*n* below the x-axis represents the number of animals, whereas the $n = 485$ within the panel is the number of individual sequences used for the analysis). Significant differences (2-tail *t* test) were observed between days 0 and 3 ($P = 0.04$) and days 3 and 5 ($P = 0.01$).

close to maximal frequencies by day 5 (87%), with little further change in the primary (93% average days 7–14) and memory (96% average) responses. Appearance of alanine or glycine at β102 follows the kinetics of the first two TCR-β chain features presented (Fig. 4 D). There is a small increase in prevalence noticeable by day 3 (33% resting to 46% by day 3) that is clearly dominant by day 5 (80%), with a further increase by day 7 (96%; 94% average, days 7–14) and little change in the memory response (97%).

The summary in Fig. 4 E presents the change in frequencies of cells that express ≥3 preferred CDR3 features across multiple animals. There is a significant increase between the resting cells and PCC-specific cells by day 3 ($P = 0.04$, 2-tail *t* test) and the greatest change between days 3 and 5 ($P = 0.01$). Although there appear to be some differences between days 5 and 7 for the individual CDR3 features discussed above, when considered together in this summary, there was no statistically significant difference. There is also no apparent difference between day 7 and week 2 of the response nor any difference between these days and the

memory response. Therefore, we conclude that a rapid maturation in the PCC-specific Th compartment for clones that express these preferred TCR-β CDR3 features is largely complete by day 5 of the primary response. We found no evidence for somatic diversification of the TCR-β chain (31) (no mutations observed for 3,406 bp analyzed for the TCR-β chain from days 7, 9, and 11; $n = 104$ single cells, 20–40 bp upstream of the CDR3 in each case).

Ag-driven Selection Rapidly Focuses the PCC-specific Response. In Fig. 5, we summarize sequence information from both chains of the TCR of single, Vα11Vβ3-expressing Th ($n = 245$; a subset of cells from Figs. 3 and 4). In the dot plot display, we emphasize the emergence of PCC-specific cells that express ≥6 of the preferred CDR3 features described above as the change in their frequency over time. Only 1/47 resting Vα11Vβ3 cells expressed ≥6 preferred CDR3 features. By day 3, 40% of the PCC-responsive compartment (Vα11Vβ3CD44^{hi}CD62L^{lo}; $n = 50$) already expressed ≥6 preferred CDR3 features. By days 5–7, this frequency doubled to 83% ($n = 59$; these days have been combined to present similar numbers in each group. There was no significant difference in frequency of cells with ≥6 preferred features between these two timepoints). There was no further change in frequency of these restricted TCR to day 14 of the primary response ($n = 43$).

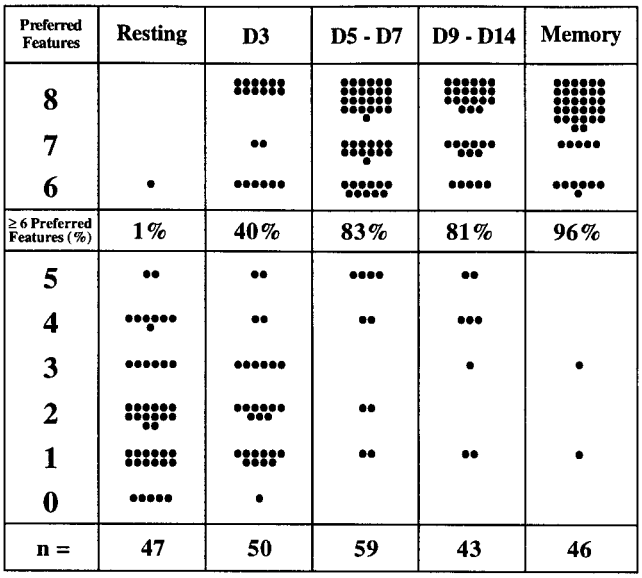

Figure 5. Ag-driven selection for preferred CDR3 features in both chains of TCR. Single-cell repertoire analysis was undertaken as described in Materials and Methods. Each dot represents the sequence information of a single cell from which both TCR-α and TCR-β were sequenced. The y-axis represents the number of preferred CDR3 features seen in each cell. Cells with ≥6 preferred features were considered as having restricted TCR, and the percentage of these cells is displayed as part of the figure (there was very little difference in the distribution of cells after day 5 of the primary response and, therefore, they were grouped to display similar *n* for each group). Sequence information from the memory response cells across days 2, 3, 4, and 6 was pooled, as these cells also displayed very little difference in the distribution of preferred features. The number of sequences used in the analysis are displayed as the *n* on the x-axis.

After secondary challenge, 96% of PCC responders expressed ≥6 preferred CDR3 features ($n = 46$). This further increase in restricted responders may indicate a separate phase of Ag-driven selection associated with the induction of a memory response. Overall, these data consider the complete TCR as the selecting unit and further attest to the rapidity of Ag-driven selection in this system.

TCR Diversity in the Early Response to Ag. Fig. 6 displays a representative set of TCR sequences from PCC-responsive, Vα11Vβ3-expressing Th from day 3 of the primary response. These sequences can be divided into three groups based on the degree of restriction in their CDR3 regions. 40% of day 3 responders expressed ≥6 CDR3 features associated with the PCC response (Fig. 6, Group 1). The second group is designated as unrestricted (containing ≤5 preferred CDR3 features), but expressed TCR-α chains similar to those sequenced from PCC-specific hybridomas, PCC-specific cell lines, or binders of moth cytochrome c (MCC)/I-E^k tetramers (Fig. 6, Group 2). Clones, such as the well-characterized 2B4, fall into this category, with a TCR-α chain that expresses none of the preferred CDR3 features we have found in the memory PCC response but is clearly specific for PCC. These first two groups account for 80% of the cells from day 3. Cells in the third group make up the remaining 20% of PCC responders from day 3 and expressed unrestricted TCR (≤5 preferred CDR3 features) that have not been previously associated with PCC specificity (Fig. 6, Group 3). It is important to note that not only was the cellular response on day 3 significantly above the adjuvant-only control (the main in vivo criteria for specificity), but the few events that were sorted from adjuvant-only controls ($n = 60$) gave rise to a PCR product with a sixfold lower efficiency (see Materials and Methods for details). The few TCR sequenced from these control populations were as diverse in their CDR3 as their preimmune counterparts (data not shown). Overall, these data indicate that PCC responders initially recruited into the immune response express more diverse TCR. Subsequently, the Th with preferred TCR are selectively expanded, and a subset of these cells are preserved for the memory response.

Ag-driven Selection Occurs Predominantly outside of the GC. We have determined that Ag-driven selection in the draining LNs is largely complete by day 5 of the primary response. In Fig. 7, we outline a quantitative analysis of the GC and non-GC distribution of PCC-specific Th over the course of the primary response. It should be noted that >90% of Vα11Vβ3-expressing T cells in the LN of B10.BR mice are CD4$^+$ Th (by flow cytometric analysis; data not shown). In Fig. 7 A, we display an example of three-color laser scanning confocal microscopic (LSCM) imaging to localize Vα11Vβ3-expressing T cells (yellow). IgD staining is used primarily to delineate B cell zone (IgD$^+$) and T cell zone (IgD$^-$) but also to locate the IgD$^-$ regions within the B cell zones that indicate the presence of GC. In Fig. 7 B, we compare our quantitation of Vα11- and/or Vβ3-expressing T cells by LSCM analysis and flow cytometry. Quantitation was undertaken from either

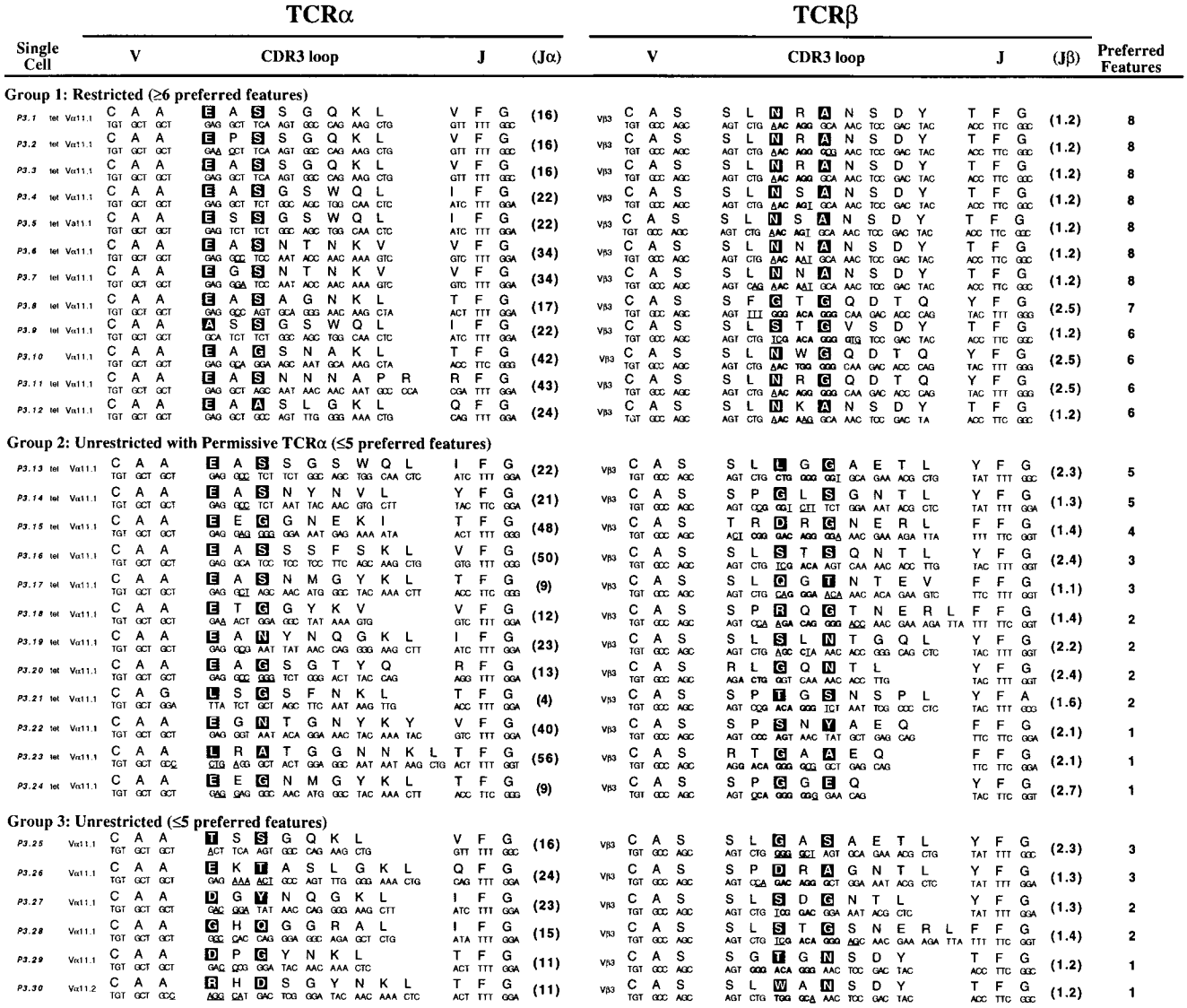

Figure 6. CDR3 diversity on day 3 of the primary response. Representative CDR3 sequence data from single, PCC-responsive T cells on day 3 of the primary response is displayed in three groups. The sequence is organized as described in Fig. 2, with TCR-α and TCR-β from each cell presented across the figure. The TCR-α aa positions α93 and α95 and the TCR-β aa positions β100 and β102 are highlighted in each sequence. Group 1 represents sequences considered to have restricted TCR (≥6 preferred features). Group 2 represents sequences that appear unrestricted (≤5 preferred CDR3 features) but where the TCR-α have at least three motifs in common with a known PCC-specific hybridoma (11, 14, 17, 32, 50) or tetramer-binding cells (tet) (McHeyzer-Williams, L.J., J.F. Panus, J.A. Mikszta, J.D. Altman, M.M. Davis, and M.G. McHeyzer-Williams, manuscript in preparation). Group 3 represents unrestricted sequences (≤5 preferred CDR3 features) that bear no resemblance to previously sequenced hybridomas in either chain of the TCR.

100,000 event flow cytometric files or cell counts from entire cross-sections of LN tissue. The concordance for proportions of the single-positive (Vα11 or Vβ3) and double-positive (Vα11Vβ3) cells within the LN populations between LSCM analysis and flow cytometry is high (Fig. 7 B). Reproducibility is also high across different animals (as indicated by the SEM; Fig. 7 B). In Fig. 7 C, the GC and non-GC distribution of Vα11Vβ3-expressing T cells across days 5, 7, and 9 is presented, and the unadjusted graphical representation of this data is shown in Fig. 8 A. From these data, it is clear that the GC reaction is in its very early stages on day 5 of the LN response, increasing by day 7 and increasing further on day 9.

Not all Vα11Vβ3-expressing T cells are PCC specific. Our flow cytometric analysis has focused on CD62L downregulation as one index for activation within the Vα11Vβ3-expressing compartment, and we can calculate the fraction of the total Vα11Vβ3 compartment that is $CD62L^{lo}$ at any stage of the response in vivo. Even at the peak of the primary response, only about half of the Vα11Vβ3-expressing cells in the draining LNs are PCC specific (by flow cytometry and TCR sequence analysis; Fig. 1). Using LSCM analysis, we demonstrate that all $V\beta3^{+}$ cells in the GC (the majority of which are $V\alpha11^{+}$; data not shown) are also $CD62L^{lo}$ (Fig. 7 D). Combining the flow cytometric and LSCM data, we can calculate the

A

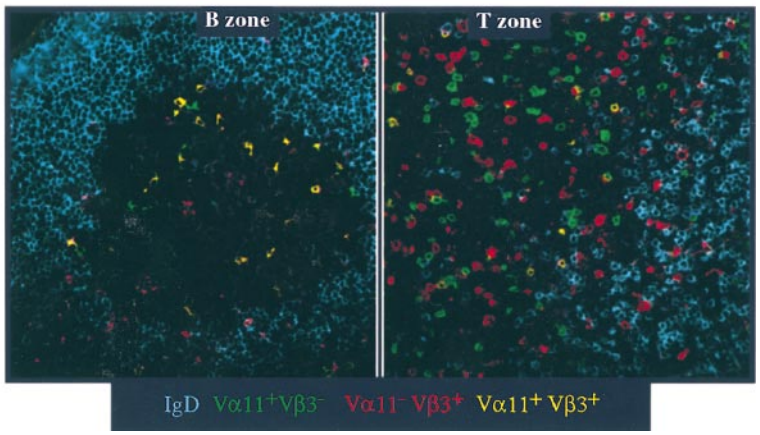

B

Phenotype	% of Total	
	Flow Cytometry	Confocal Microscopy
$V\alpha11^+V\beta3^-$	55.4 ± 0.4	53.0 ± 1.3
$V\alpha11^-V\beta3^+$	39.3 ± 0.5	41.2 ± 1.3
$V\alpha11^+V\beta3^+$	5.4 ± 0.2	5.9 ± 0.5

C

Day	Total cells counted			$V\alpha11^+V\beta3^+$ NonGC		
	$V\alpha11^+V\beta3^-$	$V\alpha11^-V\beta3^+$	$V\alpha11^+V\beta3^+$	T zone	B zone	GC
5	1360	1061	152	115	36	1
7	1241	1060	193	118	51	24
9	1484	1188	182	92	37	53

D

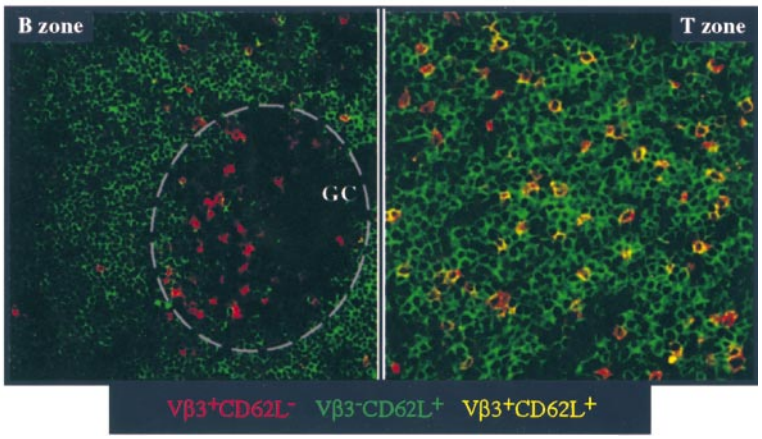

Figure 7. GC and non-GC distribution of PCC-specific Th. (A) Cryosections were prepared from the draining LNs of B10.BR mice 7 d after initial priming and stained with FITC–RR8.1 (anti-Vα11; green), allophycocyanin-KJ25 (anti-Vβ3; red), and TR-11.26 (anti-IgD; cyan). Single-color versions of the same image were collected separately (and serially in the primary detector) using LSCM analysis (40× objective lens), and then processed, colorized, and reassembled using Adobe Photoshop. IgD is used to locate the T zones (right) and B zones and GC (left panel). The cells expressing Vα11 and Vβ3 double-stain (yellow) and are more concentrated in the GC than the T zones. (B) Comparisons of Vα11Vβ3 frequencies obtained by flow cytometric analysis of total LN cells (100,000 event files; mean for four separate experiments ± SEM) and frequencies obtained by LSCM analysis (full cross-sections through LN; mean for four full sections from three separate animals ± SEM). Total numbers of Vα11 and/or Vβ3 cells are considered 100%, with the table displaying frequencies for single- and double-positive cells by each mode of analysis. (C) Summary for the distribution of Vα11Vβ3-expressing T cells over time and in three distinct locations across the draining LN. Also displayed is the total number of cells counted across three animals for each timepoint with the displayed phenotype, across three to four full cross-sections of LN. For each timepoint, the three animals pooled display little difference in distribution. (D) These day 7 primary response cryosections were stained with FITC–Mel14 (anti-CD62L; green), allophycocyanin-KJ25 (anti-Vβ3; red), and TR-11.26 (anti-IgD; not displayed. IgD^- outline of a GC is represented as a dashed circle, left). Vβ3-expressing T cells in the GC (the majority of which are also $V\alpha11^+$ in serial sections) are negative for CD62L (red in the GC; 40× objective lens), whereas the majority of T zone $V\beta3^+$ cells coexpress CD62L (right, yellow; 63× objective lens).

proportion of Vα11Vβ3 cells in the non-GC compartment that are not PCC specific. Fig. 8 B presents the adjusted distributions for PCC-specific cells over the course of the primary response and highlights the coincident decline in the non-GC compartment with the increase in the GC compartment. In Fig. 8 C, we present the expansion and decline of total PCC-specific cells (from flow cytometric data in Fig. 1 C, on a linear scale to emphasize the decline phase of the response) and then apply the frequencies of GC and non-GC Vα11Vβ3 T cells calculated by the LSCM analysis to illustrate the emergence and decline of the total PCC-specific compartment in these distinct microenvironments. We find that the plateau phase of the cellular response demonstrated by flow cytometric analysis (between days 7 and 9 of the primary response; Fig. 8 C) resolves into two peaks when the microenvironment is taken into account (Fig. 8 D). The first peak indicates maximal non-GC cell expansion (day 7), and the second peak indicates GC cell expansion (day 9). Whether these two peaks are the result of migration alone or migration and then proliferation is not clear from our data. Nevertheless, with Ag-driven selection virtually complete by day 5 of the primary response, the more delayed kinetics of the GC T cell pathway strongly argue that Ag-driven selection is a non-GC activity.

Discussion

Our study documents the evolution of clonal dominance in vivo. We believe that these processes are fundamental to the development of highly specific Th–based regulation of primary immune responses. The PCC model allows experimental access to a Th response that becomes dominated by Ag-specific Th expressing highly restricted TCR. The dominant PCC-specific cells exhibit a bias in V region usage (Vα11Vβ3) and TCR with preferred CDR3 features that provide molecular indicators of TCR diversity. In this study, we demonstrate that 70% of all $V\alpha11^+V\beta3^+$ Th ex-

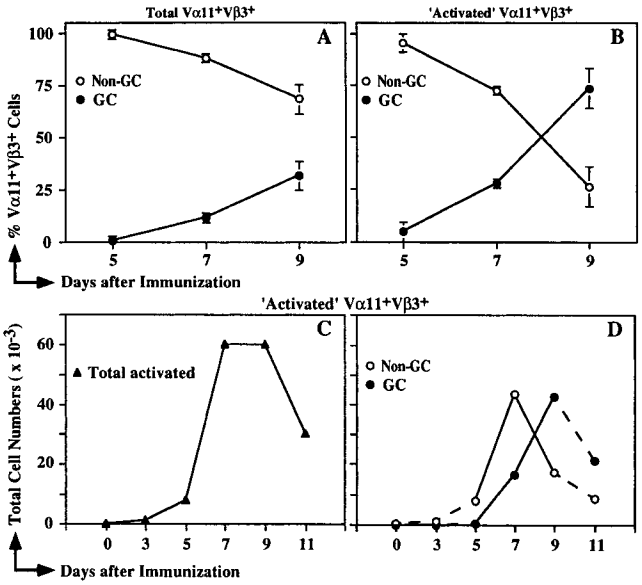

Figure 8. A shift from non-GC to GC pathway in the second week after priming. (A) Change in GC and non-GC distribution over days 5, 7, and 9 of the primary PCC response (as shown in Fig. 7 C) without adjusting for the number of Vα11Vβ3-expressing cells that do not down-regulate CD62L in response to immunization. (B) The trends in Fig. 8 A have been adjusted for mean percentage of $CD62L^{lo}$Vα11Vβ3 cells at each timepoint determined by flow cytometry (13 ± 5.1% on day 5, n = 13; 43 ± 9.4% on day 7, n = 11; and 40 ± 12% on day 9, n = 12), assuming that all GC T cells are $CD62L^{lo}$ (Fig. 7). (C) Change in total activated cells over the course of the primary response (means from Fig. 1 C) on a linear scale to emphasize the decline phase of the response. (D) Application of the frequencies shown in Fig. 8 B to estimate the change in total cell numbers in each pathway over the course of the primary response (GC are absent on day 0. In situ studies were not performed for days 3 and 11; however, to display the trends, we extrapolated day 5 frequencies to day 3 and day 9 frequencies to day 11).

press a critical PCC peptide contact residue (glutamic acid at α93), even before initial antigenic challenge. However, PCC-specific cells with all eight CDR3 features associated with the dominant clonotype only emerge to detectable levels after initial priming with PCC. Although there is some increase in the frequency of the dominant PCC-specific clonotype between the primary and memory responses (81–96%), the majority of Ag-driven selection occurs very rapidly during the first 5 d after initial priming. Clonal dominance is further propagated through selective expansion of the PCC-specific cells with the "best fit" TCR. The TCR repertoire narrows before significant GC expansion, implicating Ag and the non-GC microenvironment as the principle selecting influences in vivo.

V Region Bias in the Preimmune Repertoire. Of all eight preferred CDR3 features used by the dominant clonotype, only the glutamic acid at α93 of Vα11 preexists antigenic challenge to any significant degree. The prevalence of this residue is likely to impose the Vα11 dominance associated with PCC specificity in I-E^k–restricted animals. In PCC-specific hybridomas from many sources, Vα11 is more consistently expressed than Vβ3 (10, 11, 17, 32, 33). In studies of single chain TCR–transgenic animals, immunization with analogue peptides of MCC altered the V region dominance of PCC-specific responders (14). The Vβ3 dominance was more readily perturbed than Vα11, presumably due to modification of Ag-driven selection. Manipulations of the thymic selecting environment can also perturb V region dominance in the response to PCC. When wild-type or analogue peptides of MCC are introduced centrally, the Vβ3 dominance of MCC responders in the periphery is more noticeably affected than Vα11 (17, 32). These central manipulations are most likely to alter the availability of particular clonotypes in the preimmune repertoire rather than directly affect Ag-driven selection.

The presence of glutamic acid at α93 is not the only feature that predisposes Vα11Vβ3-expressing Th in the preimmune repertoire to bind PCC epitopes. Most Vα11Vβ3 Th on days 3 and 5 after initial priming that have not modulated CD44 or CD62L also express glutamic acid at α93. Therefore, the combination of Vα11 with the glutamic acid at α93 and any Vβ3 V region are not sufficient for PCC specificity. Furthermore, Vα11-expressing Th after PCC immunization that do not bind tetramers of MCC–I-E^k also retain a predominance of glutamic acid at α93 (67% of D8 and D14; n = 12) (McHeyzer-Williams, L.J. and M.G. McHeyzer-Williams, unpublished data). Therefore, the glutamic acid at α93 may impose the Vα11 bias seen in PCC responders, but other particular TCR features are also clearly required for fine specificity. These other features are not easily recognized in the TCR of PCC responders initially recruited in the response (isolated on day 3 of the primary). It is possible that the early responders represent a stochastic selection from the Vα11Vβ3 Th subset of preimmune Th from which the dominant clonotype is then selected. In this latter scenario, subsequent Ag-driven selection events only focus on the cells initially recruited. This would explain why there is no obvious depletion of Vα11Vβ3 Th from the nonresponder population. To argue against this stochastic model, only a minute fraction of all preimmune Vα11Vβ3 Th (0.04%) are able to bind tetramers of MCC–I-E^k (McHeyzer-Williams, L.J., J.F. Panus, J.A. Mikszta, J.D. Altman, M.M. Davis, and M.G. McHeyzer-Williams, manuscript in preparation). Overall, it is more likely that the TCR structural requirements for early recruitment into the PCC response are less stringent and, therefore, more difficult to identify.

Affinity-based Selection of Preferred CDR3 Features. TCR specificity evolves rapidly after primary exposure to Ag in vivo. By day 5 of the primary response, >80% of PCC-specific Th express restricted TCR (≥6 preferred CDR3 features). The biochemical basis for Ag-driven selection in vivo is still not clear. Lanzavecchia and colleagues demonstrate the utility of having TCR with high off-rates to enable serial triggering of multiple receptors (34, 35). In this model, lower affinity TCR receptors may be preferred and used for memory responses. In their recent study, Crawford et al. demonstrate a hierarchy of affinities for a series of PCC-specific hybridomas (using biacore analysis and correlated levels of MCC–I-E^k tetramer staining) (36). The KMAC-92 hybridoma (6/8 preferred CDR3 features) has a K_d of 29 μM (33), whereas the well-characterized 2B4 hy-

bridoma (3/8 preferred CDR3 features) has a K_d of 90 μM (37, 38). Single cells with TCR similar to 2B4 can be found early in the primary response but do not appear to be selected into the memory compartment. Furthermore, the AD10 and TCR-transgenic cells in the study by Crawford et al. (36) both express eight preferred CDR3 features (similar to the 5C.C7 TCR). Tetramers of peptide–MHC complexes have been used for analysis of class I–restricted responses in conventional animals (22, 23, 39–43) and class II–restricted responses in single-double–chain transgenic animals and T cell hybridomas (36, 44). These tetrameric reagents provide the means to assay affinity directly ex vivo in both class I– and class II–restricted responses.

Selective Expansion Propagates Clonal Dominance. Ag-driven selection of the preferred clonotypes is enhanced by selective cellular expansion in vivo. The preferred clonotype is already present on day 3 of the primary response (40% prevalence). Whether the presence of the day 3 PCC-specific cells already represents cell expansion or simply recruitment from distant sites is not yet clear. Nevertheless, the day 3 PCC-specific compartment expands a further 20-fold before reaching a plateau on day 7. Although the maximal frequency of preferred clonotypes is reached by day 5 (80%), there is still further expansion of this already restricted cell population up to day 7 (Fig. 1). Our data provides a glimpse of TCR structures that are initially recruited but are not further expanded (or preserved) in the response to PCC (day 3 sequence data; Fig. 6). Although the TCR from these early responders are less restricted than the dominant clonotype, similarly diverse CDR3 structures have been observed in the TCR-α chain of many PCC-specific hybridomas (Fig. 6, Group 2) (11, 17, 32, 33). The hybridomas have been selected in vitro, with excess amounts of specific Ag providing no selective pressure between PCC-specific clones. In contrast, there may be significant selection pressure between clones in vivo, as Ag depots recede over the course of the response. We and others have documented similar diversity in the TCR-α of T cells that bind tetramers of MCC–I-E^k (36) (McHeyzer-Williams, L.J., J.F. Panus, J.A. Mikszta, J.D. Altman, M.M. Davis, and M.G. McHeyzer-Williams, manuscript in preparation).

We see no downregulation of TCR during the PCC-specific response, as occurs in vitro after Ag stimulation (45). Although our isolation strategy clearly relies on TCR expression, there is no difference in levels of TCR between the PCC-specific cells and the nonresponder Vα11Vβ3-expressing population (data not shown). These data further argue that Ag may be limiting in vivo (at least by day 3 after initial priming). It is also possible that some Vα11Vβ3-expressing, PCC-specific clones recognize different peptide epitopes. The failure of particular clones to expand may correspond to the relative lack of availability of different epitopes over the course of the response, as suggested by Butz and Bevan for class I–restricted responses (46). It would be surprising if TCR specific for completely different epitopes used the same V region pair with similar CDR3 features. It is more likely that there may be subtle differences in the nature of the selecting peptide early in the response due to Ag processing or APC type (with different costimulatory molecules).

Clonal Selection in the Th Compartment. Our data favor a simple model of preferential clonal expansion that conforms to the edicts of the clonal selection theory (47). In this model, there is an initial recruitment of cells expressing the appropriate V region genes with particular bias toward Vα11 usage as well as Vβ3. This initial set of PCC-specific cells has more diverse TCR than the dominant clonotype but is more restricted in its CDR3 loops than in the preimmune compartment. The clones expressing all preferred TCR structures are then selectively expanded from this initial pool and dominate rapidly through cellular expansion. Both the rapid kinetics of Ag-driven selection and the highly restricted memory response suggest that focusing of TCR specificity precedes memory cell development. There is a further increase in the frequency of restricted TCR in memory responders over the late primary responders (81–96%) that could suggest another phase of selective expansion after secondary challenge. The highly restricted TCR of memory cells may underpin the rapid cellular expansion that typifies the response to secondary antigenic challenge.

Single-Cell Analysis at High Resolution. There were suggestions of clonal maturation in the Th compartment in our earlier study of the PCC response (13). The initial study suffered from two technical limitations that have been overcome in the current analysis. The first involves an emphasis on population analysis. The majority of the CDR3 sequence analysis was presented for the Vβ3 chain only, from populations of 1,000 cells as the starting point for RT-PCR. Whereas the same trends were apparent in the limited single-cell survey presented at that time ($n = 12$ from each of the primary and memory response), single-cell resolution of this study was required to provide confidence in the changes in frequency of the dominant clonotype over time (combining both cellular and molecular analyses). The second technical difficulty was the very low frequency of PCC-specific cells at the early stages of the primary response. The addition of the seventh parameter in the flow cytometric analysis reduced the background at least 10-fold. The use of an exclusion channel (excludes not only cells outside the lineage of interest but also cells that nonspecifically bind antibodies). In addition, the use of CD44 and CD62L, together with the TCR-specific reagents, greatly clarified the day 3 and 5 selection of PCC-specific cells. With this new strategy, we extended our initial survey (two timepoints, day 6 of the primary and day 6 of the memory) to the extended timecourse needed to resolve the dynamics of clonal selection in vivo.

TCR Repertoire Narrowing Precedes GC Expansion. The emergence of PCC-specific Th in the non-GC and GC microenvironments of the draining LNs of these animals is in general agreement with early studies of the splenic T cell response to this Ag (18, 28). Our analyses of repertoire narrowing are similar to the studies of Zheng et al. (18); however, the rate and extent of selection in our current study appears far more rapid. The apparent slower rate may be due to differences between the splenic and LN microenvi-

ronments that regulated these processes. Alternatively, differences may be due to the phenotypic selection used for repertoire studies in each case. The splenic PCC response also appears more restricted in the GC environment than non-GC at the same timepoint of analysis. Zheng et al. imply that Ag-driven selection is occurring in the GC and demonstrate that GC T cells are highly susceptible to CD3-mediated apoptosis resembling thymic development and selection (18). In the LN, the vast majority of Ag-driven selection is over before significant expansion of the GC compartment.

It appears unlikely that the GC reaction plays a role in the repertoire narrowing itself; it rather appears to be a site for migration of already restricted PCC-specific Th. The Ag-specific GC Th continue expanding in vivo (18, 28) and differentiate into effector cells that support the development of B cell memory (48, 49). Furthermore, we see no evidence for the somatic diversification of either chain of the TCR in this study, as previously reported (30, 31). This was also true on day 9 of the primary response, when 75% of the PCC-specific compartment resides in the GC (Fig. 8). Given the kinetics of cellular expansion in the LNs, early T zone proliferation associated with APC–Th conjugates is the most likely location for the selective expansion of preferred clonotypes (25, 27).

Conclusions. TCR specificity evolves rapidly through the preferential expansion of Ag-specific T cells well before the peak of the initial cellular response to Ag priming. These earliest events help to regulate the nature of effector cell function and shape the final specificity of the long-lived memory compartment. Here, we demonstrate not only the TCR structures of the preferred clonotypes and the kinetics of their selection, but also the TCR structures of clones initially recruited into the specific response but not expanded significantly for effector function or preserved into the memory compartment. These studies provide the framework for understanding the biochemical basis and functional consequences of maturation in the Th compartment.

We would like to thank Rebecca Caley, Gabriel Bikah, David Driver, and Garnett Kelsoe for constructive comments and critical review of the manuscript. We also thank Maria Karvelas for expert technical advice regarding confocal microscopy and the Duke Comprehensive Cancer Center Confocal Microscopy Facility. Special thanks to J. Michael Cook and the Duke Comprehensive Cancer Center Flow Cytometry Shared Resource.

J.A. Mikszta was a recipient of a National Research Service Award fellowship. This work was supported by an Arthritis Foundation Biomedical Sciences Grant and National Institutes of Health grant AI40215.

Address correspondence to Michael G. McHeyzer-Williams, Duke University Medical Center, Department of Immunology, Rm. 316 Jones Bldg., Research Dr., Durham, NC 27710. Phone: 919-613-7821; Fax: 919-684-8982; E-mail: mchey002@acpub.duke.edu

Received for publication 31 December 1998 and in revised form 19 March 1999.

References

1. Davis, M.M. 1990. T cell receptor gene diversity and selection. *Annu. Rev. Biochem*. 59:475–496.
2. Bevan, M.J. 1977. In a radiation chimaera, host H-2 antigens determine immune responsiveness of donor cytotoxic cells. *Nature*. 269:417–418.
3. Zinkernagel, R.M., G.N. Callahan, A. Althage, S. Cooper, P.A. Klein, and J. Klein. 1978. On the thymus in the differentiation of "H-2 self-recognition" by T cells: evidence for dual recognition? *J. Exp. Med*. 147:882–896.
4. Zinkernagel, R.M., and P.C. Doherty. 1974. Restriction of in vitro T cell-mediated cytotoxicity in lymphocytic choriomeningitis within a syngeneic or semiallogeneic system. *Nature*. 248:701–702.
5. Fink, P.J., and M.J. Bevan. 1978. H-2 antigens of the thymus determine lymphocyte specificity. *J. Exp. Med*. 148:766–775.
6. Ahmed, R., and D. Gray. 1996. Immunological memory and protective immunity: understanding their relation. *Science*. 272:54–60.
7. McHeyzer-Williams, M.G., J.D. Altman, and M.M. Davis. 1996. Enumeration and characterization of memory cells in the TH compartment. *Immunol. Rev*. 150:5–21.
8. Dutton, R.W., L.M. Bradley, and S.L. Swain. 1998. T cell memory. *Annu. Rev. Immunol*. 16:201–223.
9. Schwartz, R.H. 1985. T-lymphocyte recognition of antigen in association with gene products of the major histocompatibility complex. *Annu. Rev. Immunol*. 3:237–261.
10. Winoto, A., J.L. Urban, N.C. Lan, J. Goverman, L. Hood, and D. Hansburg. 1986. Predominant use of a V alpha gene segment in mouse T-cell receptors for cytochrome c. *Nature*. 324:679–682.
11. Hedrick, S.M., I. Engel, D.L. McElligott, P.J. Fink, M.L. Hsu, D. Hansburg, and L.A. Matis. 1988. Selection of amino acid sequences in the beta chain of the T cell antigen receptor. *Science*. 239:1541–1544.
12. Cochet, M., C. Pannetier, A. Regnault, S. Darche, C. Leclerc, and P. Kourilsky. 1992. Molecular detection and in vivo analysis of the specific T cell response to a protein antigen. *Eur. J. Immunol*. 22:2639–2647.
13. McHeyzer-Williams, M.G., and M.M. Davis. 1995. Antigen-specific development of primary and memory T cells in vivo. *Science*. 268:106–111.
14. Jorgensen, J.L., U. Esser, B. Fazekas de St Groth, P.A. Reay, and M.M. Davis. 1992. Mapping T-cell receptor-peptide contacts by variant peptide immunization of single-chain

transgenics. *Nature*. 355:224–230.
15. Ignatowicz, L., J. Kappler, and P. Marrack. 1996. The repertoire of T cells shaped by a single MHC/peptide ligand. *Cell*. 84:521–529.
16. Ignatowicz, L., W. Rees, R. Pacholczyk, H. Ignatowicz, E. Kushnir, J. Kappler, and P. Marrack. 1997. T cells can be activated by peptides that are unrelated in sequence to their selecting peptide. *Immunity*. 7:179–186.
17. Liu, C.-P., D. Parker, J. Kappler, and P. Marrack. 1997. Selection of antigen-specific T cells by a single IE^k peptide combination. *J. Exp. Med*. 186:1441–1450.
18. Zheng, B., S. Han, Q. Zhu, R. Goldsby, and G. Kelsoe. 1996. Alternative pathways for the selection of antigen-specific peripheral T cells. *Nature*. 384:263–266.
19. Maryanski, J.L., C.V. Jongeneel, P. Bucher, J.L. Casanova, and P.R. Walker. 1996. Single-cell PCR analysis of TCR repertoires selected by antigen in vivo: a high magnitude CD8 response is comprised of very few clones. *Immunity*. 4:47–55.
20. Busch, D.H., I.M. Pilip, S. Vijh, and E.G. Pamer. 1998. Coordinate regulation of complex T cell populations responding to bacterial infection. *Immunity*. 8:353–362.
21. Busch, D.H., and E.G. Pamer. 1998. MHC class I/peptide stability: implications for immunodominance, in vitro proliferation, and diversity of responding CTL. *J. Immunol*. 160: 4441–4448.
22. Busch, D.H., I. Pilip, and E.G. Pamer. 1998. Evolution of a complex T cell receptor repertoire during primary and recall bacterial infection. *J. Exp. Med*. 188:61–70.
23. Sourdive, D.J., K. Murali-Krishna, J.D. Altman, A.J. Zajac, J.K. Whitmire, C. Pannetier, P. Kourilsky, B. Evavold, A. Sette, and R. Ahmed. 1998. Conserved T cell receptor repertoire in primary and memory CD8 T cell responses to an acute viral infection. *J. Exp. Med*. 188:71–82.
24. Kearney, E.R., K.A. Pape, D.Y. Loh, and M.K. Jenkins. 1994. Visualization of peptide-specific T cell immunity and peripheral tolerance induction in vivo. *Immunity*. 1:327–339.
25. Khoruts, A., A. Mondino, K.A. Pape, S.L. Reiner, and M.K. Jenkins. 1998. A natural immunological adjuvant enhances T cell clonal expansion through a CD28-dependent, interleukin (IL)-2–independent mechanism. *J. Exp. Med*. 187:225–236.
26. Garside, P., E. Ingulli, R.R. Merrica, J.G. Johnson, R.J. Noelle, and M.K. Jenkins. 1998. Visualization of specific B and T lymphocyte interactions in the lymph node. *Science*. 281:96–99.
27. Ingulli, E., A. Mondino, A. Khoruts, and M.K. Jenkins. 1997. In vivo detection of dendritic cell antigen presentation to $CD4^+$ T cells. *J. Exp. Med*. 185:2133–2141.
28. Gulbranson-Judge, A., and I. MacLennan. 1996. Sequential antigen-specific growth of T cells in the T zones and follicles in response to pigeon cytochrome c. *Eur. J. Immunol*. 26:1830–1837.
29. Arden, B., S.P. Clark, D. Kabelitz, and T.W. Mak. 1995. Mouse T-cell receptor variable gene segment families. *Immunogenetics*. 42:501–530.
30. Zheng, B., W. Xue, and G. Kelsoe. 1994. Locus-specific somatic hypermutation in germinal centre T cells. *Nature*. 372: 556–559.
31. Cheynier, R., S. Henrichwark, and S. Wain-Hobson. 1998. Somatic hypermutation of the T cell receptor Vβ gene in microdissected splenic white pulps from HIV-1-positive patients. *Eur. J. Immunol*. 28:1604–1610.
32. Nakano, N., R. Rooke, C. Benoist, and D. Mathis. 1997. Positive selection of T cells induced by viral delivery of neopeptides to the thymus. *Science*. 275:678–683.
33. Liu, C.-P., F. Crawford, J. Kappler, and P. Marrack. 1998. T cell positive selection by a high density, low affinity ligand. *Proc. Natl. Acad. Sci. USA*. 95:4522–4526.
34. Valitutti, S., S. Muller, M. Cella, E. Padovan, and A. Lanzavecchia. 1995. Serial triggering of many T-cell receptors by a few peptide-MHC complexes. *Nature*. 375:148–151.
35. Viola, A., and A. Lanzavecchia. 1996. T cell activation determined by T cell receptor number and tunable thresholds. *Science*. 273:104–106.
36. Crawford, F., H. Kozono, J. White, P. Marrack, and J. Kappler. 1998. Detection of antigen-specific T cells with multivalent soluble class II MHC covalent peptide complexes. *Immunity*. 8:675–682.
37. Matsui, K., J.J. Boniface, P. Steffner, P.A. Reay, and M.M. Davis. 1994. Kinetics of T-cell receptor binding to peptide/$I\text{-}E^k$ complexes: correlation of the dissociation rate with T-cell responsiveness. *Proc. Natl. Acad. Sci. USA*. 91:12862–12866.
38. Davis, M.M., J.J. Boniface, Z. Reich, D. Lyons, J. Hampl, B. Arden, and Y.-H. Chien. 1998. Ligand recognition by αβ T Cell receptors. *Annu. Rev. Immunol*. 16:523–544.
39. Altman, J.D., P.A.H. Moss, P.J.R. Goulder, D.H. Barouch, M.G. McHeyzer-Williams, J.I. Bell, A.J. McMichael, and M.M. Davis. 1996. Phenotypic analysis of antigen-specific T lymphocytes. *Science*. 274:94–96.
40. Murali-Krishna, K., J.D. Altman, M. Suresh, D.J. Sourdive, A.J. Zajac, J.D. Miller, J. Slansky, and R. Ahmed. 1998. Counting antigen-specific CD8 T cells: a reevaluation of bystander activation during viral infection. *Immunity*. 8:177–187.
41. Flynn, K.J., G.T. Belz, J.D. Altman, R. Ahmed, D.L. Woodland, and P.C. Doherty. 1998. Virus-specific $CD8^+$ T cells in primary and secondary influenza pneumonia. *Immunity*. 8:683–691.
42. Gallimore, A., A. Glithero, A. Godkin, A.C. Tissot, A. Pluckthun, T. Elliott, H. Hengartner, and R. Zinkernagel. 1998. Induction and exhaustion of lymphocytic choriomeningitis virus–specific cytotoxic T lymphocytes visualized using soluble tetrameric major histocompatibility complex class I–peptide complexes. *J. Exp. Med*. 187:1383–1393.
43. Bousso, P., A. Casrouge, J.D. Altman, M. Haury, J. Kanellopoulos, J.-P. Abastado, and P. Kourilsky. 1998. Individual variations in the murine T cell response to a specific peptide reflect variability in naive repertoires. *Immunity*. 9:169–178.
44. Gutgemann, I., A.M. Fahrer, J.D. Altman, M.M. Davis, and Y.-H. Chien. 1998. Induction of rapid T cell activation and tolerance by systemic presentation of an orally administered antigen. *Immunity*. 8:667–673.
45. Valitutti, S., S. Muller, M. Salio, and A. Lanzavecchia. 1997. Degradation of T cell receptor (TCR)–CD3-ζ complexes after antigenic stimulation. *J. Exp. Med*. 185:1859–1864.
46. Butz, E.A., and M.J. Bevan. 1998. Massive expansion of antigen-specific $CD8^+$ T cells during an acute virus infection. *Immunity*. 8:167–175.
47. Burnet, F.M. 1959. The Clonal Selection Theory of Acquired Immunity. Cambridge University Press, Cambridge, UK.
48. Han, S., K. Hathcock, B. Zheng, T.B. Kepler, R. Hodes, and G. Kelsoe. 1995. Cellular interactions in germinal centers: roles for CD40 ligand and B7-2 in establishing germinal centers. *J. Immunol*. 155:556–567.
49. van Essen, D., H. Kikutani, and D. Gray. 1995. CD40 ligand-transduced co-stimulation of T cells in the development of helper function. *Nature*. 378:620–623.
50. Kaye, J., M.L. Hsu, M.E. Sauron, S.C. Jameson, N.R. Gascoigne, and S.M. Hedrick. 1989. Selective development of $CD4^+$ T cells in transgenic mice expressing a class II MHC-restricted antigen receptor. *Nature*. 341:746–749.